

Can heterogeneous core–mantle electromagnetic coupling control geomagnetic reversals?

Daniel Brito^{*}, Jonathan Aurnou, Peter Olson

Johns Hopkins University Baltimore, MD 21218-2681, USA

Received 12 June 1998; received in revised form 3 November 1998; accepted 4 November 1998

Abstract

An analytical model is developed for the electromagnetic torques exerted on the mantle by the poloidal magnetic field of the core interacting with a laterally heterogeneous conducting layer at the base of the mantle. Torques due to changes in both orientation and intensity of a dipolar poloidal field are included. Contrary to earlier suggestions, our calculations predict that the trajectory of the magnetic pole during a polarity reversal is not strongly affected by heterogeneity in mantle electrical conductivity. © 1999 Elsevier Science B.V. All rights reserved.

Keywords: Geomagnetic field; Polarity Reversals; Core–mantle coupling; Electromagnetic torques; D'' structure

1. Introduction

The behavior of the geomagnetic field during polarity reversals is critical for understanding the geodynamo and the coupling between the core and mantle. If the core and mantle were entirely decoupled, the long-term behavior of the geodynamo and its history of polarity reversals would have no relationship to the three-dimensional structure of the mantle. This does not seem to be the case. There is

both observational evidence as well as theoretical support for the concept that mantle heterogeneity influences geomagnetic reversals.

The best known and most controversial evidence for a mantle influence are the numerous paleomagnetic studies reporting longitudinal confinement of transitional Virtual Geomagnetic Pole (VGP) positions, primarily from deep sea sediment records (Tric et al., 1991; Clement, 1991; Clement et al., 1995). Perhaps the most striking evidence is the compilation by Laj et al. (1991) of deep sea sediment VGPs from the past 12 million years, indicating a preference for two reversal paths, one beneath the Americas and one beneath Asia, the two separated by nearly 180° in longitude. The paths coincide with regions of anomalously high seismic velocity in the lower man-

^{*} Corresponding author. Present address: LGIT, Obs. de Grenoble, Grenoble, France.

tle, suggesting a connection with the structure and perhaps the dynamics of the lower mantle.

The veracity of this interpretation has been questioned, particularly from studies of reversals using directional data obtained from lavas. Comparably sized data sets from lavas have failed to show the same amount of longitudinal confinement (Valet et al., 1992; Prevot and Camps, 1993; Courtillot and Valet, 1995; Hoffman, 1995). Possible explanations for VGP paths include biases in site distribution for deep sea sediment records or biases in the sediment recording process (Quidelleur and Valet, 1994; Channell and Lehman, 1997). Alternatively, it has been suggested that deviations of the transition field from dipolar symmetry might produce an apparent longitude confinement as an artifact (Gubbins and Coe, 1993; Barton and McFadden, 1996). But even the lava data shows some longitudinal preference, when a more uniformly-distributed sampling of recording sites is made (Love, 1998).

There is additional evidence from the geomagnetic field on shorter time-scales indicating influence of mantle heterogeneity. Johnson and Constable (1995, 1997) have constructed models of the time-averaged paleofield for the past 5 million years which indicate that certain structures seen in the historical field, most notably the equatorially symmetric flux lobes at high latitudes and the difference in secular variation between Pacific and Atlantic hemispheres, persist over that time interval. Using a combination of archeomagnetic, dated lavas and recent sediment data, Constable et al. (1996) have modeled the paleomagnetic field at 100-year intervals for the past 3000 years and find evidence for these same non-dipole features.

In addition to the evidence from geomagnetic and paleomagnetic data, our present knowledge of the structure of the mantle and our present understanding of mantle and core dynamics both suggest that the mantle should influence the behavior of the geodynamo, including the frequency and style of polarity reversals. The wide spectrum of lateral heterogeneity in the D'' region at the base of the mantle indicates that dynamical effects such as heat flow and critical physical properties such as conductivity vary significantly on the mantle side of the core–mantle boundary (CMB) (Loper and Lay, 1995; Lay et al., 1998). Mantle heterogeneity can affect polarity reversals in

several ways, including thermal interaction between core and mantle, in which heat flow variations on the CMB provide the coupling of the magnetic field to mantle structure and electromagnetic interaction, in which heterogeneity in electrical conductance above the CMB provides the coupling.

Thermal coupling has already been investigated using numerical calculations of thermal convection in rotating fluid spheres driven by heterogeneous temperature or heterogeneous heat flow conditions applied on the outer boundary (Zhang and Gubbins, 1993; Olson and Glatzmaier, 1996). The main result of these calculations is that CMB thermal heterogeneity perturbs the pattern of convection in the core by adding a component of flow that is locked to mantle structure. Dynamo calculations in which the flow pattern is kinematically locked to mantle structure exhibit pole path confinement during polarity reversals (Gubbins and Sarson, 1994). The fully dynamic dynamo calculations show a more complex response to mantle heterogeneity (Glatzmaier et al., 1997). Non-axisymmetric heterogeneity in boundary heat flow increases the level of time variability of the convection in the calculations, which in turn controls the frequency of polarity reversals, but not their paths.

A second form of heterogeneous core–mantle interaction that might affect reversals is based on electromagnetic coupling. This mechanism has received far less attention. Runcorn (1992, 1996) emphasized the fundamental differences between thermal and electromagnetic coupling, by pointing out that heterogeneous electromagnetic coupling is not expected to lock the core to the mantle during constant polarity epochs but only during polarity transitions, when the field is highly asymmetric with respect to the spin axis. Instead of altering the pattern of core convection, electromagnetic torques act to rotate the core into a preferred orientation during a polarity change, causing the transition field to appear biased toward mantle structure. Runcorn also pointed out that this mechanism can be understood using simple models of the transition field. Unlike thermal coupling, it requires only minimal assumptions about the structure of the geomagnetic field and the underlying cause of reversals.

Other types of torques could affect the reversal process, including torques from mechanical friction,

from the interaction of pressure variations in the core fluid with topography on the core–mantle boundary (Hide, 1969; Jault and Le Mouél, 1989; Greff-Lefftz and Legros, 1995), and from gravitational torques between the mantle and the inner core (Xu and Szeto, 1994; Buffett, 1996a,b). We do not consider these in this paper. Instead, we focus on Runcorn's mechanism by extending the model of Aurnou et al. (1996) for electromagnetic confinement of the VGP longitude during magnetic reversals. In addition to the electromagnetic torques induced by changes in field intensity, we include the torques generated by motion of the VGP and by mantle leakage of the core toroidal field into the D''-layer, as well as core–mantle inertia. We make use of a thin layer approximation to obtain analytical solutions for the differential rotation of the core and mantle during a reversal, in the presence of conductivity variations in the D''-layer similar to the three-dimensional seismological structure of the lowermost mantle. Contrary to Runcorn (1996) and Aurnou et al. (1996), we find that lateral variations in electrical conductance in D'' does not by itself produce longitudinally confined VGPs.

2. Core–mantle electromagnetic torques with mantle heterogeneity

In this section we derive general expressions for electromagnetic torques due to the magnetic field of the core acting on conductivity heterogeneity at the base of the mantle. The poloidal field of the core generates currents in the conductive D''-layer through two different mechanisms. First, time variations of the radial field intensity at the CMB induce electrical currents in D''. Interaction of a non-axisymmetric magnetic field with the induced currents generates Lorentz forces and a torque on the mantle usually referred to as the poloidal torque (Stix and Roberts, 1984). The mechanism is illustrated in Fig. 1a for the particular case of an inclined decaying dipolar magnetic field. This couple causes differential rotation of the core and the mantle. Second, motion of the core field relative to the mantle shears the magnetic field and generates electrical currents in the conducting

D''-layer, the so-called ω -effect (Moffatt, 1978). Electromagnetic torques on the mantle produced this way are usually referred to as toroidal torques. This mechanism is illustrated in Fig. 1b.

As shown in Fig. 2, our model consists of (i) the conducting fluid core which is the source of the poloidal magnetic field; (ii) the thin, heterogeneous, electrically conducting D''-layer just above the CMB which is in electrical contact with the core; (iii) the rest of the mantle, treated as electrically insulating. We assume that the fluidity of the outer core permits the core and its magnetic field to rotate with respect to the mantle about the polar axis (see Fig. 2). This relative rotation is affected by the polar component of the electromagnetic torque acting between the core and mantle.

Seismic studies of the CMB region indicate substantial lateral heterogeneity near the base of the mantle that could produce large variations in electrical conductance. Garnero and Helmberger (1996) have identified discrete regions a few tens of kilometers thick at the base of the mantle with anomalously slow P-wave velocities. Within these regions, which range in thickness from 0 to 40 km, the P-wave velocity is reduced by nearly 10% relative to the overlying mantle. This basal layer is thick beneath the central Pacific, where global seismic tomography indicates lower than average seismic velocities for the lower mantle, and is missing or undetected beneath the circum-Pacific ring of higher-than-average lower mantle velocities (Lay et al., 1998; Garnero et al., 1998).

The inverse correlation between the thickness of the basal layer and large-scale heterogeneity in the lower mantle is precisely what is expected for a dense, chemically distinct layer at the base of the mantle. A dense basal layer is predicted from mantle convection dynamics to be thickest beneath lower mantle upwellings and thin or absent beneath lower mantle downwellings (Kellogg and King, 1993; Kellogg, 1997). The composition of this layer is uncertain, although there are only two viable possibilities: partial melting and iron enrichment, with partial melting providing a somewhat better match to the observations (Williams and Garnero, 1996). Either of these two would imply enhanced electrical conduction (Jeanloz, 1993) although the magnitude is uncertain (Poirier and Le Mouél, 1992).

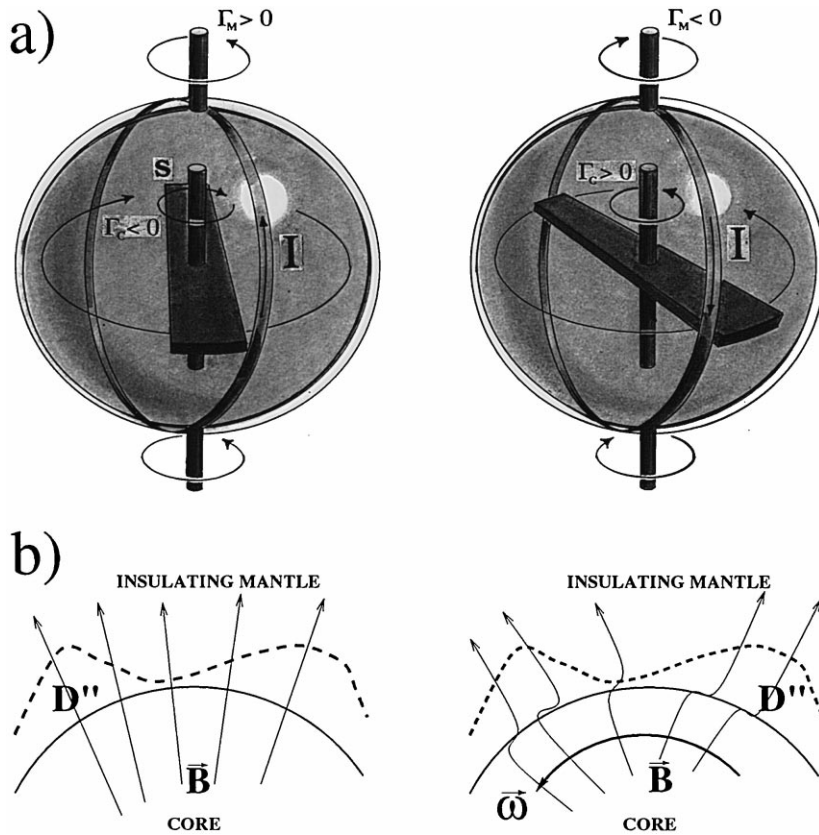


Fig. 1. Sketches illustrating two different mechanisms for generating an electromagnetic torque on the mantle by heterogeneity in the D'' -layer. (a) Electrical currents I are induced in the mantle by decay of an inclined core field, represented by a bar magnet. Misalignment of the magnetic field and the current caused by mantle heterogeneity generates an axial torque on the mantle Γ_M , and an opposite torque on the core Γ_C tending to rotate the pole of the field perpendicular to the loop of current. (b) Shearing of the poloidal magnetic field by motion relative to the heterogeneous conducting D'' -layer. Thickness variations in D'' -layer are represented by a dashed line. In this case the torque resists the motion.

Since the large-scale pattern of lower mantle heterogeneity is dominated by spherical harmonic degree 2 pattern (Loper and Lay, 1995) we adopt the following simplified representation of the D'' -layer thickness variations:

$$D(\theta, \phi) = \bar{D} + D_0 \sin^2 \theta \cos 2\phi \quad (1)$$

where \bar{D} is the mean thickness of D'' and D_0 is the amplitude of the D'' -layer thickness variations. According to the results of Garnero and Helmlinger (1996), \bar{D} and D_0 are both approximately 20 km. Accordingly, we use a value of 20 km for \bar{D} and D_0 in the following calculations.

In order to simplify the analysis, we suppose that the conductivity of the D'' -layer is small compared to the core conductivity, e.g., $\sigma_D/\sigma_C \ll 1$ where σ_D is the electrical conductivity in D'' and σ_C is the electrical conductivity in the core (see Table 1). To first order in this ratio, the poloidal magnetic field in the mantle $r \geq r_C$ can be expressed in terms of a scalar potential,

$$p_o(r, \theta, \phi) = r_E \sum_{n=1}^{\infty} \sum_{m=0}^n \frac{1}{n} \left(\frac{r_E}{r} \right)^{n+1} P_n^m(\cos \theta) \times (g_n^m \cos m\phi + h_n^m \sin m\phi) \quad (2)$$

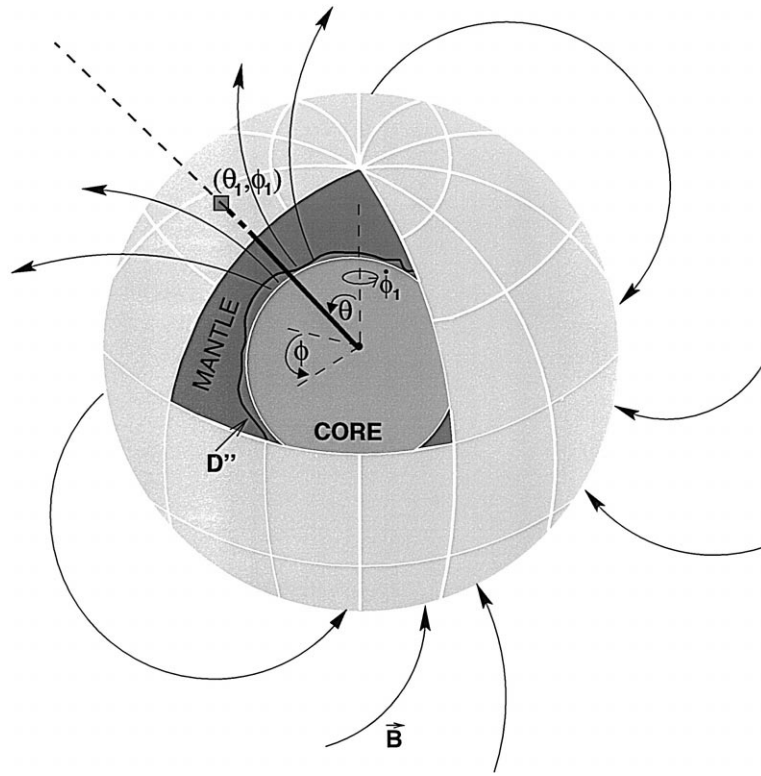


Fig. 2. Illustration of the model geometry, showing the field lines of an inclined dipolar magnetic field permeating the laterally heterogeneous conducting D''-layer at the base of the mantle. The position of the north magnetic pole of the field is (θ_1, ϕ_1) . The angular rotation rate of the core relative to the mantle is $\dot{\phi}_1$ assuming the magnetic field rotates with the core.

where r_E is the radius of the Earth, (g_n^m, h_n^m) are the Gauss coefficients (Merrill et al., 1996), P_n^m are the

associated Legendre polynomials with the Schmidt normalization and (r, θ, ϕ) are spherical coordinates.

Table 1
Quantities used in torque estimates

Symbol	Quantity	Units	Value
I_R	Reduced moment of inertia	kg m ²	8.3×10^{36}
I_C	Core moment of inertia	kg m ²	9.2×10^{36}
I_M	Mantle moment of inertia	kg m ²	8.0×10^{37}
r_C	Core radius	m	3.48×10^6
r_E	Earth radius	m	6.37×10^6
μ_0	magnetic permeability	H m ⁻¹	$4\pi \times 10^{-7}$
σ_C	Core conductivity	S m ⁻¹	3×10^5
σ_D	D''-layer electrical conductivity	S m ⁻¹	$\sim 3 \times 10^3$
\bar{D}	Averaged D'' thickness	m	2×10^4
D_0	Variations in D'' thickness	m	2×10^4
B	Typical poloidal magnetic field intensity	mT	0.37
B_0	Magnetic field strength before reversal	mT	0.37
dT/dr	Toroidal field gradient on CMB	T m ⁻¹	-1×10^{-9}
k_{dipole}	Dipole decay time	years	$\sim 15,000$

The radial component of a dipole field at the CMB is, using (2),

$$B_r(r_C, \theta, \phi, \theta_1, \phi_1) = 2 \left(\frac{r_E}{r_C} \right)^3 (g_1^0 \cos \theta + g_1^1 \sin \theta \cos \phi + h_1^1 \sin \theta \sin \phi) \quad (3)$$

with

$$\begin{cases} g_1^0(\theta_1, \phi_1) = \frac{1}{2} \left(\frac{r_C}{r_E} \right)^3 B \cos \theta_1 \\ g_1^1(\theta_1, \phi_1) = \frac{1}{2} \left(\frac{r_C}{r_E} \right)^3 B \sin \theta_1 \cos \phi_1 \\ h_1^1(\theta_1, \phi_1) = \frac{1}{2} \left(\frac{r_C}{r_E} \right)^3 B \sin \theta_1 \sin \phi_1 \end{cases} \quad (4)$$

and

$$B = 2 \left(\frac{r_E}{r_C} \right)^3 \sqrt{(g_1^0)^2 + (g_1^1)^2 + (h_1^1)^2} \quad (5)$$

where r_C is the radius of the core and (θ_1, ϕ_1) is the north magnetic pole of the dipole on the CMB.

The electromagnetic torque vector on the mantle is given by (Rochester, 1962)

$$\vec{\Gamma}_M = \int_{V_M} \vec{r} \times (\vec{J} \times \vec{B}) dV \quad (6)$$

where \vec{r} is the radius vector, $\vec{J} = (J_r, J_\theta, J_\phi)$ is the electrical current density vector in the mantle, $\vec{B} = (B_r, B_\theta, B_\phi)$ is the magnetic field vector and the integration extends over the electrically conducting part of the mantle V_M . We are only concerned with the polar component of the torque, the component Γ_M about the mantle rotation axis:

$$\Gamma_M = \int_{V_M} (J_r B_\theta - J_\theta B_r) r \sin \theta dV \quad (7)$$

2.1. Torque from time variations of the poloidal field

To compute the poloidal torque resulting from dipole field intensity variations, we introduce the poloidal potential p

$$\vec{B} = \nabla \times \nabla \times (\vec{r}p) \quad (8)$$

Following Holme (1998), (7) becomes

$$\Gamma_P = \int_{V_M} \frac{1}{\mu_0} L^2 p \frac{\partial(\nabla^2 p)}{\partial \phi} dV \quad (9)$$

where Γ_P is the poloidal torque acting on the mantle and

$$L^2 = - \left[\frac{1}{\sin \theta} \frac{\partial}{\partial \theta} \left(\sin \theta \frac{\partial}{\partial \theta} \right) + \frac{1}{\sin^2 \theta} \frac{\partial^2}{\partial \phi^2} \right] \quad (10)$$

is the quantum mechanical angular momentum operator (Arfken, 1985). Following Stix and Roberts (1984), we write $p = p_0 + p_1 + \dots$ where p_1 is a small perturbation of the core field p_0 . In V_M , p_0 obeys $\nabla^2 p_0 = 0$ and p_1 obeys

$$\frac{\partial p_0}{\partial t} = \frac{1}{\mu_0 \sigma_D} \nabla^2 p_1 \quad (11)$$

Then using (9) and (11), the mantle torque from time variations of the poloidal magnetic field is

$$\Gamma_P = \int_{V_M} \sigma_D L^2 p_0 \frac{\partial^2 p_0}{\partial t \partial \phi} dV \quad (12)$$

In order to evaluate the torque (12) in presence of lateral heterogeneity in conductivity, we assume that the mantle conductivity is zero everywhere except in D'' , and that the D'' -layer can be approximated as a thin conductive layer in electrical contact with the core with a variable thickness $D(\theta, \phi)$ (see Eq. (1)). The following conditions allow us to treat D'' as locally uniform

$$D(\theta, \phi) \ll r_C, \quad \frac{1}{r_C} \frac{\partial D(\theta, \phi)}{\partial \theta} \ll 1,$$

$$\frac{1}{r_C \sin \theta} \frac{\partial D(\theta, \phi)}{\partial \phi} \ll 1 \quad (13)$$

and, therefore, J_θ is also locally uniform in the D'' -layer. With the approximation in (13), we can integrate (12) radially from the CMB to the top of

D''-layer to obtain the following approximate surface integral

$$\Gamma_P = \oint_{\text{CMB}} \left[L^2 p_0 \frac{\partial^2 p_0}{\partial t \partial \phi} \right]_{r=r_C} C(\theta, \phi) dS \quad (14)$$

where the D'' conductance is defined by

$$C(\theta, \phi) = \int_{r_C}^{r_C + D(\theta, \phi)} \sigma_D(r, \theta, \phi) dr. \quad (15)$$

In the simplified case of a uniform conductivity in D'', (14) reduces to

$$\Gamma_P = \sigma_D \oint_{\text{CMB}} \left[L^2 p_0 \frac{\partial^2 p_0}{\partial t \partial \phi} \right]_{r=r_C} D(\theta, \phi) dS. \quad (16)$$

2.2. Torque from shear of the poloidal field

Differential rotation of the core and mantle shears the poloidal field across the CMB, inducing a secondary component of the magnetic field b_ϕ and a toroidal torque as illustrated in Fig. 1b. Using the continuity of the tangential component of the electrical field at the CMB, we obtain, for uniform differential rotation and uniform mantle conductivity

$$b_\phi(r, \theta, \phi) = \mu_0 \sigma_D r_C B_r(r_C, \theta, \phi) \times [r - (r_C + \bar{D})] \dot{\phi}_1 \sin \theta$$

for $r_C < r < r_C + \bar{D}$ (17)

and

$$J_\theta(\theta, \phi) = -\frac{1}{\mu_0} \frac{\partial b_\phi}{\partial r} = -\sigma_D r_C B_r(r_C, \theta, \phi) \dot{\phi}_1 \sin \theta$$

for $r_C < r < r_C + \bar{D}$ (18)

where $\dot{\phi}_1$ is the azimuthal angular velocity of the core relative to the mantle.

Substitution of (18) into (7) and integration in radius yields the toroidal torque Γ_T due to the shearing of the poloidal magnetic field

$$\Gamma_T = 4\sigma_D \dot{\phi}_1 \oint_{\text{CMB}} [p_0^2]_{r=r_C} D(\theta, \phi) \sin^2 \theta dS. \quad (19)$$

2.3. Torque from leaking toroidal field

There is another electromagnetic torque sometimes used to explain length of day variations, the

Table 2
Estimates of Torque Magnitudes

Torque	Definition	Magnitude [N m]
Γ_{P1}	Dipole decay	10^{16}
Γ_{P2}	Dipole ϕ -motion	10^{17}
Γ_{P3}	Dipole θ -motion	10^{16}
Γ_T	CMB shear	10^{19}
Γ_{motion}	$\Gamma_{P2} + \Gamma_T$	10^{19}
Γ_{leakage}	B_T diffusion	10^{19}

so-called ‘leakage’ torque. This torque arises from the diffusion of the toroidal field at the CMB into the D''-layer. For an azimuthal toroidal field $B_T \hat{\phi}$ the leakage currents associated with this field are

$$J_r = \frac{1}{\mu_0} \left[\frac{1}{r} \frac{B_T}{\tan \theta} + \frac{1}{r} \frac{\partial B_T}{\partial \theta} \right] \quad (20)$$

$$J_\theta = -\frac{1}{\mu_0} \left[\frac{B_T}{r} + \frac{\partial B_T}{\partial r} \right] \quad (21)$$

In the thin layer approximation, $\partial B_T / \partial r$ dominates. Following Stix and Roberts (1984) we write

$$B_T = T(r) \sin 2\theta \quad (22)$$

and assume $dT/dr \approx -1 \times 10^{-9} \text{ T m}^{-1}$ on the CMB. Using (1), (3), (7) and (22), we find that the interaction between the leakage toroidal field and the dipolar poloidal field produces the torque

$$\Gamma_{\text{leakage}} = \frac{1}{\mu_0} r_C^3 \frac{16\pi}{15} \bar{D} \left[\frac{dT}{dr} \right]_{r=r_C} B \cos \theta_1 \quad (23)$$

Using the parameter values in Table 1, expression (23) indicates that the leakage torque is roughly comparable in amplitude to the poloidal or toroidal torques that we will calculate in the following sections (see Table 2). However, it depends only on the averaged value \bar{D} and not on the lateral heterogeneities of the D''-layer. Accordingly, the leakage torque does not tend to lock the core to mantle heterogeneity and thus will not come into play in the reversal models described below.

3. Reversal models

3.1. The decaying field model

Here we consider the response of a stationary inclined dipolar magnetic field in free decay. Paleo-

magnetic intensity estimates indicate that the field intensity typically decays by a factor of 2 to 10 in a geomagnetic reversal prior to the directional change (Valet and Meynadier, 1993). To model this phase of the reversal process, we define (5) as

$$B = 2 \left(\frac{r_E}{r_C} \right)^3 \sqrt{(g_0^1)^2 + (g_1^1)^2 + (h_1^1)^2} = B_0 e^{-kt} \quad (24)$$

where k is the decay factor and B_0 is the initial strength of the poloidal field (see Table 1). Then substituting (1), (3) and (24) into (16), we find the poloidal torque for an inclined dipole with pole at (θ_1, ϕ_1) is

$$\Gamma_{P1}(\theta_1, \phi_1, t) = -\sigma_D r_C^4 D_0 \frac{4\pi}{15} B_0^2 k e^{-2kt} \times [\sin^2 \theta_1 \sin 2\phi_1] \quad (25)$$

Note that the electromagnetic torque originating from the spherically-symmetric conductance \bar{D} is zero and

only lateral variations in D'' conductance contribute to (25).

Fig. 3 shows the variations of Γ_{P1} as a function of the pole position. When the pole lies in a region where the torque is positive, the mantle is accelerated and the core decelerated by the electromagnetic couple. The opposite effect occurs when the pole lies in a region where the torque is negative. The pole tends to drift in longitude when it lies below these regions of the mantle, in the directions indicated in Fig. 4. Separating the positive and negative torque regions are curves where the torques on both the core and mantle vanish, representing the locus of possible equilibrium positions for an inclined field during free decay. However, only two of the four zero-torque curves, the ones drawn in heavy bold lines in Fig. 3 and in solid lines in Fig. 4, represent stable equilibria. The electromagnetic couple attracts the pole when it is in the neighborhood of these curves. Conversely, the electromagnetic couple tends to repel the pole from the neighborhood of the other two zero torque curves. This is the mechanism described by Aurnou et al. (1996) and is a modified version of the Runcorn conjecture: an inclined dipole

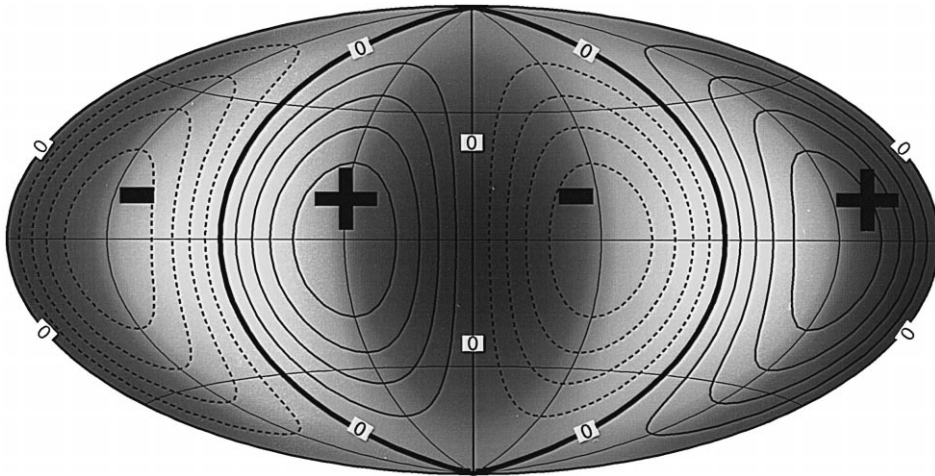


Fig. 3. Axial component of the electromagnetic torque Γ_{P1} exerted on the mantle as a function of the position of the pole of the magnetic field (θ_1, ϕ_1) , computed assuming the thickness of the electrically conducting D'' -layer varies as $P_2^2(\cos \theta)$ (shaded contours). Line contours indicate torque variations. Shaded contours indicate D'' -thickness variations with dark shading representing thick and light representing thin regions of D'' , respectively. Two zero-torque contours (bold curves) define the locus of dynamically stable pole positions. The other two zero-torque contours define the locus of dynamically unstable pole positions, and coincide with the thin regions of D'' .

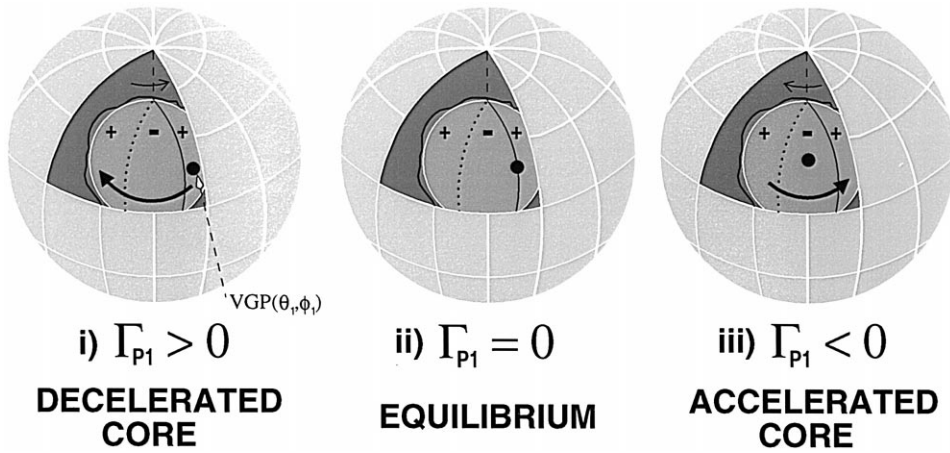


Fig. 4. Explanation of the core–mantle differential rotation driven by the electromagnetic torque Γ_{P1} . \cdot is the instantaneous position of the VGP of the transitional field. Positive (+) and negative (–) signs on the CMB are the signs of Γ_{P1} , the electromagnetic torque applied on the mantle for a given position of the VGP. Case (i): Γ_{P1} is positive, the mantle is accelerated (thin arrow) and the core is decelerated (thick arrow). The VGP drifts to the west toward the zero torque position. Case (ii): The VGP is located where $\Gamma_{P1} = 0$. In this position the VGP is stable to longitude perturbations. The other zero torque curve (dashed line) is an unstable position. Case (iii): Γ_{P1} is negative. The mantle is decelerated (thin arrow) and the core is accelerated (thick arrow). The VGP drifts to the east toward the zero torque position.

is stable at longitudes $\phi_1 = 90^\circ$ and $\phi_1 = 270^\circ$ close to the longitudinal bands identified by Laj et al. (1991). According to our parametrization of the heterogeneous D'' -layer, the stable longitude bands at $\phi = 90^\circ$ and 270° correspond to regions of low electrical conductivity within D'' . Thus, when the magnetic field is in decay, the effect of Γ_{P1} is to push the inclined magnetic pole away from areas of high electrical conductivity in D'' , towards areas of low electrical conductivity.

Neither Aurnou et al. (1996) or Runcorn (1996) considered the electromagnetic torques that accompany the motion of the pole. When these are included the conclusions are different. Two additional torques arise when the core and the magnetic field rotate at an azimuthal angular velocity $\dot{\phi}_1$ relative to the mantle. The first is due to variations in poloidal magnetic flux at the CMB accompanying the motion of the magnetic pole position. Using (1), (2) and (16) with $dg_1^1/dt = (\partial g_1^1/\partial \phi_1)\dot{\phi}_1$ and $dh_1^1/dt = (\partial h_1^1/\partial \phi_1)\dot{\phi}_1$, we obtain for this torque

$$\Gamma_{P2} = \sigma_D r_C^4 B^2 \frac{2\pi}{15} \left[5\bar{D}[\sin^2\theta_1] + 2D_0[\sin^2\theta_1 \cos 2\phi_1] \right] \dot{\phi}_1 \quad (26)$$

The second torque is due to the shear of the magnetic field at the CMB. Using (1), (2) and (19), we obtain for this toroidal torque

$$\Gamma_T = \sigma_D r_C^4 B^2 \left[\frac{8\pi}{15} \bar{D} [1 + \sin^2\theta_1] + \frac{16\pi}{35} D_0 [\sin^2\theta_1 \cos 2\phi_1] \right] \dot{\phi}_1 \quad (27)$$

The total torque on the mantle from differential rotation between the mantle and core is the sum of the two contributions:

$$\Gamma_{\text{motion}} = \Gamma_{P2} + \Gamma_T = \left[\sigma_D r_C^4 B^2 \frac{2\pi}{15} \left(\bar{D} [4 + 9\sin^2\theta_1] + \frac{38}{7} D_0 [\sin^2\theta_1 \cos 2\phi_1] \right) \right] \dot{\phi}_1 \quad (28)$$

Since the bracketed term in (28) is positive, this torque is always resistive. Thus the poloidal torque induced from changes in the magnetic flux through D'' and the toroidal torque due to shear of the

magnetic field lines in D'' -layer both oppose any differential rotation between the mantle and the core.

The driving torque Γ_{P1} and the resistive torque Γ_{motion} enter the angular momentum balance for motion of the core with respect to the mantle reference frame

$$-(\Gamma_{P1} + \Gamma_{\text{motion}}) = I_R \frac{d\dot{\phi}_1}{dt} \quad (29)$$

where the left-hand side represents the sum of the axial torques acting on the core, I_R is the reduced moment of inertia of the core and $\dot{\phi}_1$ is the angular azimuthal rotation rate of the core relative to the mantle. The reduced moment of inertia of the core is defined as $I_R = I_M I_C / (I_M + I_C)$ where I_C is the moment of inertia of the core and I_M is the moment of inertia of the mantle (see Table 1).

Numerical solutions of (29) show that after an initial transient adjustment, a steady state appears where the rotation rate of the core relative to the mantle becomes constant (Brito, 1998). This steady state can be obtained analytically by setting the sum of the torques in (29) to zero, using (25) and (28). The result is

$$\dot{\phi}_{1,\text{steady}} = \frac{(\sin^2\theta_1 \sin 2\phi_1)}{\left[2 + \frac{9}{2}\sin^2\theta_1 + \frac{19}{7}\sin^2\theta_1 \cos 2\phi_1\right]} k \quad (30)$$

Using the slowest decay mode for a dipole magnetic field in a sphere, $k_{\text{dipole}} = \pi^2 / (\mu_0 \sigma_C r_C^2)$, gives

$$\dot{\phi}_{1,\text{steady}} \approx 6 \times 10^{-4} \text{ deg/year} \quad (31)$$

where we have taken $\theta_1 = 90^\circ$ and $\phi_1 = 45^\circ$. At this rate the core would require at least 150,000 years to rotate through $\delta\phi_1 = 90^\circ$. With such a slow response, the amount of differential rotation between core and mantle during a typical 10,000 year polarity change is only a few degrees.

No pole paths are found when the motional torques are taken into account. The torques that result from the motion of the core magnetic field relative to the conducting layer at the base of the mantle strongly resist any change in the VGP longitude. Our results show that the motional torques will always dominate the driving torque due to mantle heterogeneity. The results in (30) and (31) also show that the value of

$\dot{\phi}_{1,\text{steady}}$ does not depend on the value of the electrical conductivity in the D'' -layer.

3.2. Paths of a rotating dipole

A second calculation examines a model similar to Runcorn's, in which the intensity of the transition dipole field remains constant and the pole rotates in latitude at a constant rate $\dot{\theta}_1$. Using (1), (2) and (16) with $dg_1^1/dt = (\partial g_1^1/\partial\theta_1)\dot{\theta}_1$ and $dh_1^1/dt = (\partial h_1^1/\partial\theta_1)\dot{\theta}_1$, the axial poloidal torque on the mantle becomes

$$\Gamma_{P3} = \left(\sigma_D r_C^4 B^2 \frac{2\pi}{15} D_0 [\sin 2\theta_1 \sin 2\phi_1]\right) \dot{\theta}_1 \quad (32)$$

As in the previous case, we set the sum of the two torques (28) and (32) to zero and obtain the steady state differential rotation of the core:

$$\dot{\phi}_{1,\text{steady}} = - \frac{(\sin 2\theta_1 \sin 2\phi_1)}{\left[4 + 9\sin^2\theta_1 + \frac{38}{7}\sin^2\theta_1 \cos 2\phi_1\right]} \dot{\theta}_1 \quad (33)$$

In this case the differential rotation rate is proportional to the reversal speed $\dot{\theta}_1$. However the proportionality factor is small, of order 0.11 for $\theta_1 = \phi_1 = 45^\circ$. According to (33), we expect a maximum longitude deflection of only about 10° as the pole rotates through 180° of latitude.

In the ideal case where we set $\Gamma_{\text{motion}} = 0$, the stable pole paths for Γ_{P3} are located along $\phi_1 = 90^\circ, 270^\circ$ in the northern hemisphere and $\phi_1 = 0^\circ, 180^\circ$ in the southern hemisphere. Therefore, continuous longitudinal pole paths do not exist for a dipole field rotating in latitude. The effect of Γ_{P3} is to repel the VGP from high conductivity regions while the core is rotating towards the equator and then to attract the VGP to high conductivity regions when the core is rotating away from the equator. The model of Runcorn (1996) predicts that the rotating dipole will always be repelled from the high conductivity regions in the lowermost mantle. Our models differ because we assume that D'' is electrically connected to the core, whereas Runcorn (1996) assumed that the core and the conductive regions in the lower mantle were not in electrical contact.

4. Conclusions

We have developed an approximate analytical model for core–mantle electromagnetic coupling with a heterogeneous D'' -layer. The model includes resistive torques as well as the driving torques considered previously by Runcorn (1992, 1996) and Aurnou et al. (1996). We find that the resistive torques dominate the response of the core–mantle system to changes in the core magnetic field, irrespective of the value of the electrical conductivity in D'' . Our calculations of core–mantle electromagnetic coupling with various transition magnetic field configurations indicate that the effects of lateral variations in electrical conductance in the D'' -layer are generally too weak to cause much differential rotation of the core relative to the mantle on the time-scale of a typical magnetic polarity reversal. Indeed, we find that the main effect of electromagnetic coupling between the core and the mantle, even coupling via heterogeneity in D'' -layer, is to inhibit changes in the longitude of an inclined magnetic pole. Electromagnetic torques tend to constrain the VGP at the same longitude during reversals. Thus the rapid longitudinal swings of the VGP recorded in some reversal records is a behavior that is inconsistent with electromagnetic coupling.

Acknowledgements

We would like to thank R. Holme, D. Jault, P. Roberts for many helpful discussions and M. Alexandrescu and an anonymous reviewer for constructive remarks. Support from the Geophysics Program of the NSF is gratefully acknowledged.

References

Arfken, G., 1985. *Mathematical Methods for Physicists*. Academic Press, San Diego.

Aurnou, J.M., Buttles, J.L., Neumann, G.A., Olson, P.L., 1996. Electromagnetic core–mantle coupling and paleomagnetic reversal paths. *Geophys. Res. Lett.* 23, 2705–2708.

Barton, C.E., McFadden, P.L., 1996. Inclination shallowing and preferred transitional VGP paths. *Earth Planet. Sci. Lett.* 140, 147–157.

Bruto, D., 1998. *Approches expérimentales et théoriques de la dynamique du noyau terrestre: Tourbillon géostrophique de gallium liquide dans un champ magnétique, anisotropie et rotation de la graine, chemins d'inversion*. Université Paris VII, PhD thesis, 305 pp.

Buffett, B.A., 1996a. Gravitational oscillations in the length of day. *Geophys. Res. Lett.* 23, 2279–2282.

Buffett, B.A., 1996b. A mechanism for decade fluctuations in the length of day. *Geophys. Res. Lett.* 23, 3803–3806.

Channell, J.E.T., Lehman, B., 1997. The last two geomagnetic reversals recorded in high-deposited-rate sediments drift. *Nature* 389, 712–715.

Clement, B.M., 1991. Geographical distribution of transitional VGPs: evidence for non-zonal equatorial symmetry during Matuyama–Brunhes geomagnetic reversal. *Earth Planet. Sci. Lett.* 104, 48–58.

Clement, B.M., Rodda, P., Smith, E., Sierra, L., 1995. Recurring transitional geomagnetic field geometries. *Geophys. Res. Lett.* 22, 3171–3174.

Constable, C.G., Johnson, C.L., Lund, S.P., 1996. 3000 Years of quasi-global geomagnetic secular variation. *EOS Trans. Am. Geophys. Union* 77, 143.

Courtilot, V., Valet, J.P., 1995. Secular variation of the Earth's magnetic field: from jerks to reversals. *C.R. Acad. Sci. Paris* 320, 903–922.

Garnero, E.J., Helmberger, D.V., 1996. Seismic detection of a thin laterally varying boundary layer at the base of the mantle beneath the Central-Pacific. *Geophys. Res. Lett.* 23, 977–980.

Garnero, E.J., Revenaugh, J., Williams, Q., Lay, T., Kellogg, L., 1998. Ultra-low velocity zone at the core–mantle boundary. In: Gurnis, M., Buffett, B.A., Knittle, E., Wyssession, M. (Eds.), *The Core–Mantle Boundary*. Am. Geophys. Union.

Glatzmaier, G.A., Roberts, P.H., Coe, R.S., 1997. Studying reversal frequency with geodynamo simulations. *EOS Trans. Am. Geophys. Union* 77, 195.

Greff-Leffitz, M., Legros, H., 1995. Core–mantle coupling and polar motion. *Phys. Earth Planet. Inter.* 91, 273–283.

Gubbins, D., Coe, R.S., 1993. Longitudinally confined geomagnetic reversal paths from non-dipolar transition fields. *Nature* 362, 51–53.

Gubbins, D., Sarson, G., 1994. Geomagnetic field morphologies from a kinematic dynamo model. *Nature* 368, 51–55.

Hide, R., 1969. Interaction between the Earth's liquid core and solid mantle. *Nature* 222, 1055–1056.

Hoffman, K., 1995. Dipolar reversal states of the geomagnetic field and core–mantle dynamics. *Nature* 359, 789–794.

Holme, R., 1998. Electromagnetic core–mantle coupling: I. Explaining decadal changes in the length of day. *Geophys. J. Int.* 132, 167–180.

Jault, D., Le Mouél, J.L., 1989. The topographic torque associated with a tangentially geostrophic motion at the core surface and inferences on the flow inside the core. *Geophys. Astrophys. Fluid Dyn.* 48, 273–296.

Jeanloz, R., 1993. Chemical reactions at the Earth's core–mantle boundary: summary of evidence and geomagnetic implications. In: *Relating Geophysical Structures and Processes: The Jeffreys Volume*. AGU Geophys. Monograph 76, 121–127.

- Johnson, C.L., Constable, C.G., 1995. The time-averaged geomagnetic field as recorded by lava flows over the past 5 Ma. *Geophys. J. Int.* 122, 489–519.
- Johnson, C.L., Constable, C.G., 1997. The time-averaged geomagnetic field: global and regional biases for 0–5 Ma. *Geophys. J. Int.* 131, 643–666.
- Kellogg, L.H., 1997. Growing the Earth's D''-layer layer: effects of density variations at the core–mantle boundary. *Geophys. Res. Lett.* 24, 2749–2752.
- Kellogg, L.H., King, S., 1993. Effect of mantle plumes on the growth of D'' by reaction between the core and mantle. *Geophys. Res. Lett.* 20, 379–382.
- Laj, C., Mazaud, A., Weeks, R., Fuller, M., Herrero-Berverra, E., 1991. Geomagnetic reversal paths. *Nature* 351, 447.
- Lay, T., Williams, Q., Garnero, E.J., 1998. The core–mantle boundary layer and deep Earth dynamics. *Nature* 392, 461–468.
- Loper, D., Lay, T., 1995. The core–mantle boundary region. *J. Geophys. Res.* 100, 6397–6420.
- Love, J.J., 1998. Paleomagnetic volcanic data and geomagnetic regularity of reversals and excursions. *J. Geophys. Res.* 103 (12), 435–12452.
- Merrill, R.T., McElhinny, M.W., McFadden, P.L., 1996. *The Magnetic Field of the Earth*. Academic Press, London.
- Moffatt, H.K., 1978. *Magnetic Field Generation in Electrically Conducting Fluids*. Cambridge Univ. Press, New York.
- Olson, P.L., Glatzmaier, G.A., 1996. Magnetoconvection and thermal coupling of the Earth's core and mantle. *Phil. Trans. R. Astron. Soc. A* 354, 1413–1424.
- Poirier, J.P., Le Mouél, J.L., 1992. Does infiltration of core material into the lower mantle affect the observed geomagnetic field?. *Phys. Earth Planet. Inter.* 73, 29–37.
- Prevot, M., Camps, P., 1993. Absence of preferred longitude sectors for poles from volcanic records of geomagnetic reversals. *Nature* 366, 56–57.
- Quidelleur, X., Valet, J.P., 1994. Paleomagnetic records of excursions and reversals: possible biases caused by magnetization artefacts. *Phys. Earth Planet. Inter.* 8, 27–48.
- Rochester, M.G., 1962. Geomagnetic core–mantle coupling. *J. Geophys. Res.* 67, 4833–4836.
- Runcorn, S.K., 1992. Polar path in geomagnetic reversals. *Nature* 356, 654–656.
- Runcorn, S.K., 1996. Preferred paths of VGPs in geomagnetic reversal records and their significance. *Surveys in Geophys.* 17, 229–232.
- Stix, M., Roberts, P.H., 1984. Time-dependent electromagnetic core–mantle coupling. *Phys. Earth Planet. Inter.* 36, 49–60.
- Tric, E., Laj, C., Jehanno, C., Valet, J.P., Kissel, C., Mazaud, A., Iccarino, S., 1991. High resolution record of the Upper Olduvai Transition from Po Valley (Italy) sediments: support for dipolar transition geometry?. *Phys. Earth Planet. Inter.* 65, 319–336.
- Valet, J.P., Meynadier, L., 1993. Geomagnetic field intensity and reversals during the past four million years. *Nature* 336, 234–238.
- Valet, J.P., Tucholka, P., Courtillot, V., Meynadier, L., 1992. Paleomagnetic constraints on the geometry of the geomagnetic field during reversals. *Nature* 356, 400–407.
- Williams, Q., Garnero, E.J., 1996. Seismic evidence for partial melt at the base of Earth's mantle. *Science* 273, 1528–1530.
- Xu, S., Szeto, A.M.K., 1994. Gravitational coupling in the Earth's interior revisited. *Geophys. J. Int.* 118, 94–100.
- Zhang, K.K., Gubbins, D., 1993. Convection in a rotating spherical fluid shell with an inhomogeneous temperature boundary condition at infinite Prandtl number. *J. Fluid Mech.* 250, 209–232.